ARTICLE

Check for updates

Ancient and recent collisions revealed by phosphate minerals in the Chelyabinsk meteorite

Craig R. Walton [1✉], Oliver Shorttle[1,2], Sen Hu [3], Auriol S. P. Rae[1], Ji Jianglong [3], Ana Černok [4], Helen Williams[1], Yu Liu [5], Guoqiang Tang[5], Qiuli Li [5] & Mahesh Anand [4]

The collision history of asteroids is an important archive of inner Solar System evolution. Evidence for these collisions is brought to Earth by meteorites. However, as meteorites often preserve numerous impact-reset mineral ages, interpretation of their collision histories is controversial. Here, we combine analysis of phosphate U-Pb ages and microtextures to interpret the collision history of Chelyabinsk—a highly shocked meteorite. We show that phosphate U-Pb ages correlate with phosphate microtextural state. Pristine phosphate domain U-Pb compositions are generally concordant, whereas fracture-damaged domains universally display discordance. Combining both populations best constrains upper (4473 ± 11 Ma) and lower intercept (−9 ± 55 Ma, i.e., within error of present) U-Pb ages. All phosphate U-Pb ages were completely reset during an ancient high energy collision, whilst fracture-damaged domains experienced further Pb-loss during mild and recent collisional re-heating. Targeting textural sub-populations of phosphate grains permits more robust reconstruction of asteroidal collision histories.

[1] Department of Earth Sciences, University of Cambridge, Downing Street, Cambridge CB2 3EQ, UK. [2] Institute of Astronomy, University of Cambridge, Madingley Road, Cambridge CB3 OHA, UK. [3] Key Laboratory of Earth and Planetary Physics, Institute of Geology and Geophysics, Chinese Academy of Sciences, 100029 Beijing, China. [4] School of Physical Sciences, Open University, Walton Hall, Milton Keynes MK7 6AA, UK. [5] State Key Laboratory of Lithospheric Evolution, Institute of Geology and Geophysics, Chinese Academy of Sciences, 100029 Beijing, China. ✉email: crw59@cam.ac.uk

ollisions play a fundamental role in shaping rocky objects in our Solar System by (i) building protoplanets[1], (ii) replenishing or eroding planetary atmospheres[2], and (iii) violently perturbing surface environments[3]. Collisions shape surfaces through cratering; transforming the mineralogy and texture of affected rocks by shock metamorphism, and driving diffusive resetting of radioisotope mineral ages through post-shock thermal metamorphism[4]. Crustal records of impact bombardment on the Earth, Moon, and Mars have been used to validate dynamical models of Solar System evolution[5,6], but suffer from the effects of planetary resurfacing in deeper time.

Asteroids provide an alternative record of collisional events in the inner Solar System[7]. Unlike planets, asteroids have been thermally quiescent (cold) since around 4500 Ma[8]. Therefore, any mineral ages younger than the end of parent body metamorphism should faithfully record impact-induced metamorphism. Phosphate minerals represent a wide-spread class of low-to-medium closure temperature U–Pb geochronometers found in meteorites, with which we can sample the asteroid collisional record. Age clusters in the meteorite phosphate U–Pb record have been linked to the formation of Earth's Moon[7,9], the migration of giant planets[10], and the recent to long-term evolution of the asteroid belt[11–16]. Constraints on key events in Solar System and Earth history are therefore written in the collision histories of meteorites. However, this seemingly ideal data set is compromised by ambiguity in the interpretation of upper versus lower concordia intercept phosphate U–Pb ages: specifically, the question of whether or not high energy collisions are needed to induce Pb-loss from the phosphate crystal lattice[17].

This ambiguity is exemplified by Chelyabinsk: an ordinary chondrite shocked meteorite sampling the LL asteroid, not affected by terrestrial alteration[18] (Fig. 1). Chelyabinsk (Fig. 1a) represents an allochthonous (formed from mobilised material), proximal impactite (short transport distance from point of impact), clast-rich (containing pieces of host-rock material) melt rock, sometimes known as impact-melt breccia[19]. Melt rocks are formed during high-velocity collisions, which deliver sufficient energy to induce extensive melting of the target object (Fig. 1b)[20]. Chelyabinsk preserves three lithologies: light (host rock), dark (containing a higher proportion of melted phases), and shock melt (fully melted and quench crystallised material) (Fig. 1c). Phosphates in the dark lithology experienced peak temperatures at least 200 K higher than those in the light lithology, whilst phosphates in the melt lithology were destroyed[21–23] (Fig. 1).

The simplest interpretation of these observations is that all three lithologies were produced together during a single impact event: light lithology fragments were entrained in shock melt and the dark lithology formed by the interaction between the two, as both individual isolated blocks and as cooked margins around larger light lithology fragments[18,24,25] (Fig. 1). However, both previously reported upper (4456 ± 18 Ma) and lower (559 ± 180 Ma) intercept phosphate U–Pb ages for Chelyabinsk[26,27] have been individually suggested to record the same high-energy event of simultaneous melting and brecciation. Furthermore, numerous other ages are obtained using different mineral chronometers[24,26,28–31] (Supplementary Fig. 18). This level of ambiguity in the collisional chronology of shocked meteorites draws a veil over key events in Solar System history, which could otherwise be constrained using
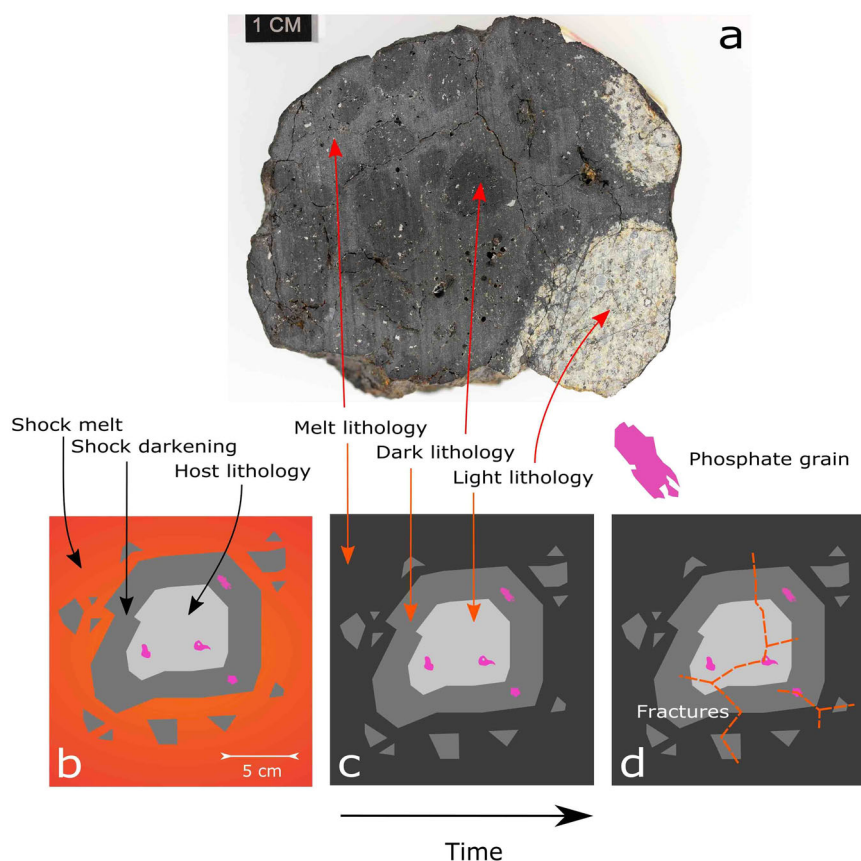
Fig. 1 Rock textures in Chelyabinsk. a–d Evolution of Chelyabinsk breccia (**a**), from (**b**) initial formation during shock-melting, brecciation, and shock darkening of host rock material, through (**c**) solidification into light, dark, and melt lithologies, and (**d**) subsequent minor disturbances, such as the propagation of fracture networks. Pink symbols represent host-rock phosphate minerals, which are only found in the light and dark lithologies. Photograph used is of Chelyabinsk specimen NHMV-O707; Credit Ludovic Ferriére-NHM Vienna, Austria.
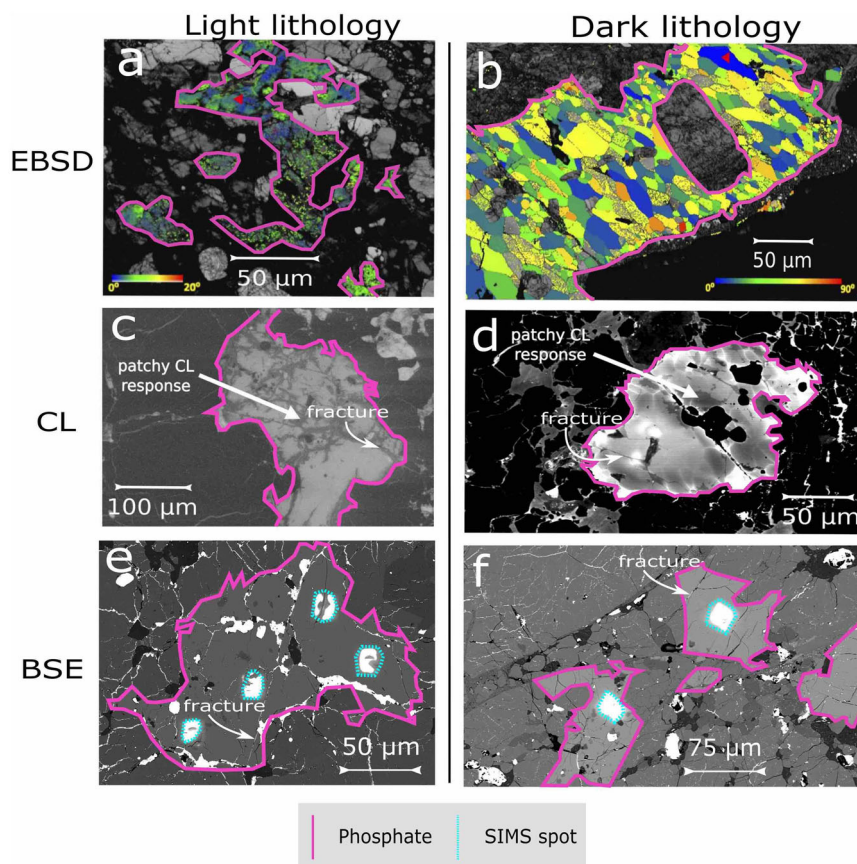
Fig. 2 Mineral microtextures in Chelyabinsk. In EBSD images, colour-scheme indicates crystal lattice misorientation relative to an arbitrary point (red triangle). **a** apatite grain showing smooth gradations in lattice misorientation, revealing strain and associated deformation. This strain was most plausibly accumulated during impact. **b** merrillite grain with distinct subgrains of uniform and unstrained crystal lattice orientation, revealing recrystallisation that likely developed in response to more extensive heating. **c** apatite showing patchy CL response, correlated with fractures. **d** merrillite showing subgrain recrystallisation, as well as overprinting patchy CL response correlated with fractures. **e** apatite showing extensive fracturing. Metal and sulfide veins (white in BSE image) fill some fractures, whereas others are unfilled. **f** apatite grain showing similar fracturing, proximal to a shock melt-vein. Partially annealed metal and sulfide veins are abundant in the silicate matrix. In all images, phosphates are outlined in purple. Pole figures and further data related to panels a and b are available in Supplementary Fig. 16.

phosphate mineral ages. To address this deficit, we require a better understanding of the phosphate texture-age record of asteroids.

Mineral microtextures provide geological context for spatially resolved radioisotope ages, e.g., crystal structural integrity, which can influence Pb diffusion[32]. Microtextures are increasingly being targeted to reduce uncertainty in the interpretation of spatially resolved phosphate U–Pb ages[33–37]. We have previously conducted a detailed microtextural survey of phosphate minerals in the Chelyabinsk meteorite[21]. Here, we present an in-situ U–Pb dating study of texturally-distinct phosphate populations in the meteorite, allowing us to re-interpret the collision history of Chelyabinsk and its parent body. We utilise Scanning Electron Microscopy (SEM), Electron Back Scattered Diffraction (EBSD), Cathodoluminescence (CL), and Secondary Ionisation Mass Spectrometry (SIMS) analyses to assess the phosphate texture-age record of Chelyabinsk (see Methods). We further verify our interpretative model by making and testing predictions for the wider meteoritic phosphate texture-age record.

Results and discussion
Microtextural evidence for recent and ancient collisions. The light and dark lithologies of Chelyabinsk each preserve grains of the phosphate minerals apatite ($Ca_5(PO_4)_3[OH, Cl, F]$) and merrillite ($Ca_9NaMg(PO_4)_7$). Previous EBSD analyses[21] have revealed that all light lithology phosphate grains display domains of distorted crystal orientation, which is most likely attained during a crystal-plastic recovery process (Fig. 2a), whereas dark lithology merrillites display randomly oriented strain-free sub-domains (Type II recrystallisation)[38], evidencing recrystallisation likely driven by more intensive heating (Fig. 2b). This specific association of phosphate textures with lithology type suggests the formation of the Chelyabinsk melt rock during a *single impact event*—an interpretation which is supported by similar observations made for phosphates in terrestrial impactites[25].

The strain-free domains of dark lithology merrillite indicate minimal post-recrystallisation deformation. However, CL images, which are sensitive to phosphate trace element composition[34], reveal patchy textures correlated with fractures, which are clearly visible in Back Scatter Electron (BSE) images (Fig. 2c–f). These features evidence a later low energy event, which affected individual grains in both the light and dark lithology, regardless of their microtextural state (Fig. 2c, d). We refer to grain domains with a high area-density of fractures and associated patchy CL zones as damaged crystal domains, and those without pristine crystal domains. Phosphate microtextural evidence therefore records distinct high-temperature pathways in the dark and light lithologies during primary impact, whilst shared patchy CL textures (Fig. 2c, d) and fracture networks (Fig. 2e, f) indicate equivalent later (minor) shock histories[21].
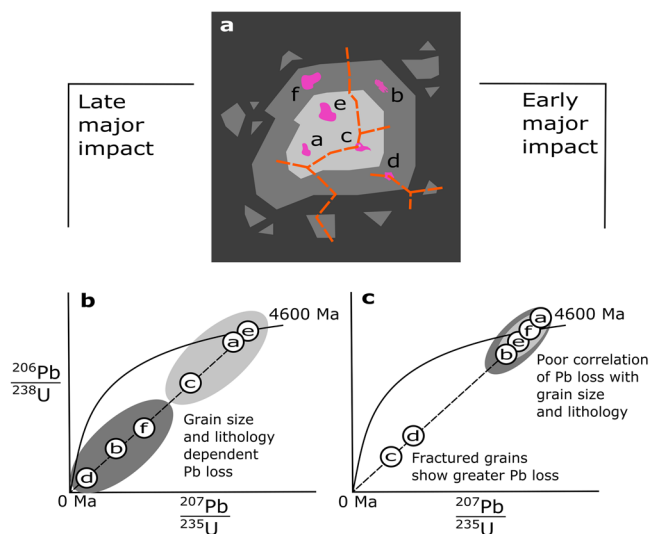
Fig. 3 Scenarios for Pb-loss from Chelyabinsk phosphates during impact. a Schematic view of phosphate grain populations in Chelyabinsk lithologies. Small and large pristine phosphate grains are shown, as well as grains with fracture-damaged domains. **b** If recent Pb-loss corresponds to a major event of shock metamorphism and post-shock heating, Pb should diffuse more rapidly from smaller grains, and from those grains hosted in the dark lithology (higher peak temperature). **c** If recent Pb-loss corresponds to a relatively mild heating event that only noticeably affected fractured-damaged grains, Pb-loss will have been stochastic, possibly independent of grain size, occurred throughout both lithologies equally, and will be more developed in fracture-damaged rather than pristine grain populations. Colour-scheme interpretation is the same as in Fig. 1d.

Possible scenarios of age resetting. Lead diffusion in apatite is strongly temperature dependent[39]. Complete diffusion and loss of Pb will also occur faster for smaller crystals. The deformed and recrystallised populations of phosphates in Chelyabinsk experienced different thermal histories (Fig. 1), and have grain sizes (maximum width) that vary from sub-micron (below minimum detection size by EBSD) to several hundred micrometres throughout each lithology (Fig. 2). These observations allow us to test different hypotheses regarding the nature and timing of collisions recorded by Chelyabinsk (Fig. 3).

If recent shock and post-shock thermal metamorphism were responsible for simultaneously inducing strain, recrystallisation, and U–Pb discordance in Chelyabinsk phosphates, we predict that Pb-loss should be significantly more extensive in the more intensely shocked and heated dark lithology phosphates[17,38], as well as in smaller grains (Fig. 3b). Conversely, late Pb-loss may be unrelated to the development of Chelyabinsk's primary shock textures, and may instead record a milder recent thermal event. In this case, we predict that Pb-loss should be uncorrelated with phosphate location in Chelyabinsk light or dark lithology (Fig. 3c). This holds because (1) to the extent that phosphate populations were only partially reset during an initial energetic collision, billions of years of subsequent radiogenic decay will have greatly reduced space on the concordia plot between grain populations that experienced Pb-loss early; and (2) reverse discordance induced in late events may have further blurred the original data distributions of light versus dark lithology phosphates.

For comparison, mild temperatures which are insufficient to drive Pb diffusion from pristine zicon ($ZrSiO_4$) crystal lattice may be sufficient to drive Pb-loss from damaged zircon grains[32,40]. Much as in metamict zircons that do not experience annealing,

then, phosphate crystal domains damaged by fractures may be susceptible to a late episode of Pb-loss at only mild temperature conditions. In this scenario, we predict that damaged crystal domains will display more extensive Pb-loss, or discordance, whilst pristine domains will be broadly concordant (Fig. 3c). These hypotheses allow us to use textural and chronometric relationships to constrain the timing and nature of collisional events affecting the Chelyabinsk melt breccia.

Statistical analysis of phosphate U–Pb data. Our results allow us to test the scenarios presented in Fig. 3 for late Pb-loss in response to either (1) a primary impact event, with Pb-loss principally occurring in dark lithology grains that experienced more intensive heating, or (2) a mild secondary event, with Pb-loss principally occurring in damaged grains in both lithologies. Regressions of U–Pb data split by lithology and by microtextural state are shown in Fig. 4.

We find no correlation of phosphate discordance with U-content or grain size in Chelyabinsk (Supplementary Figs. 10–15). We tested the null hypothesis that there is no difference in Pb-loss between each phosphate population using Two-sided Kolmogorov–Smirnov (KS) tests of $\frac{207Pb}{235U}$ data distributions. Light and dark lithology grain populations are statistically identical in this test (Fig. 4c), whereas pristine and fracture-damaged populations are highly significantly different (Fig. 4d). Our results support a scenario in which Pb-loss occurred mainly in fracture-damaged grains as a result of a late impact event, which only produced mild pressures and temperatures in the Chelyabinsk material.

There is then the question of how best to regress phosphate population data and interpret the resulting concordia intercept ages (Fig. 4). At the 2 σ level, upper and lower intercept age uncertainties obtained using light and dark lithology or pristine and fracture-damaged phosphate populations overlap (Fig. 4). Pristine domains yield a well-defined upper-intercept age (4453 ± 36 Ma) as well as a weakly constrained lower intercept age (696 ± 813 Ma). Fracture-damaged phosphate crystal domains yield a similarly well-constrained upper-intercept age (4477 ± 12 Ma) and a much more tightly constrained lower intercept age (−3 ± 56 Ma, i.e., recent, within error of the present day). We used F-tests to test the null hypothesis that all data should be regressed together, rather than being regressed as sub-populations. Results reveal that treating light and dark and pristine and fractured phosphate populations separately during regression is not statistically justified at 99% confidence (Table S1). Pristine and fracture-damaged grains therefore serve to constrain different regions along a single linear regression, together yielding our preferred intercept ages of 4473 ± 11 Ma and −9 ± 55 Ma. This upper-intercept age is statistically identical to those previously reported for Chelyabinsk, whilst our revised lower intercept is several hundred Myr younger than previously reported ages[26,27].

Interpretation of U–Pb regressions and intercept ages. The revised lower intercept obtained after identifying and including damaged phosphate domains in a phosphate U–Pb age calculation for Chelyabinsk appears to have geological significance. Lower intercepts may be of dubious meaning when no concordant data is observed[32]. However, many pristine phosphate domains display fully concordant spot data (Fig. 4b). Multiple episodes of partial Pb-loss from damaged grains, which would greatly complicate any interpretation, should manifest as U–Pb spots that fall off the regression line[32]. However, isotope data for damaged crystal domains are well described by a single linear regression (Fig. 4b). We conclude that the youngest and most
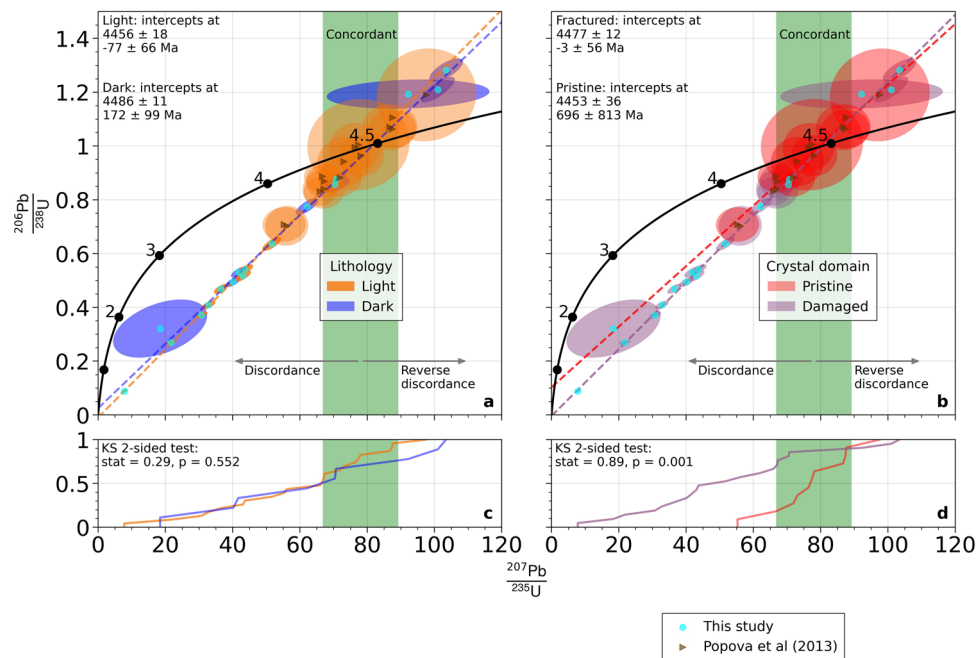
Fig. 4 Statistics and concordia chronology of phosphates in Chelyabinsk. Each data point is shown with shaded 1σ error ellipse. **a** Comparison of light and dark lithology phosphate grain populations. **b** Comparison of pristine and damaged phosphate crystal domain analyses. **c** Statistical comparison of Cumulative Distribution Function (CDF) plots of $\frac{207Pb}{235U}$ ratios for light and dark lithology phosphate data. The populations cannot be statistically resolved using two-sided Kolmogorov-Smirnov tests. **d** Statistical comparison of CDFs for pristine and damaged phosphate crystal domain data. The populations are statistically resolved, with the pristine population having higher Pb/U than the damaged grain population. Regression using all data best constrains upper (4473 ± 11 Ma) and lower intercept (−9 ± 55 Ma ages).

tightly constrained U–Pb lower intercept age defined by fracture-damaged phosphates in Chelyabinsk most plausibly reflects Pb loss from damaged grains during a comparatively minor shock and reheating event in the geologically recent past[32,40] (Fig. 3c).

The large uncertainty on the lower intercept age obtained using pristine phosphate domains alone (Fig. 4b) suggests that fracture-damaged phosphate grains must be identified and used in the regression in order to properly constrain lower intercept ages. Given that the preferred Chelyabinsk upper-intercept U–Pb age of all phosphate domains presented here (4473 ± 11 Ma) is younger than the time that primitive asteroids cooled below the Pb diffusion closure temperature for phosphate minerals (Fig. 5), and given the similar degree of partial Pb loss from phosphates in both lithologies, all phosphate U–Pb ages must initially have been fully reset during a primary impact event (Fig. 5). Partial Pb loss must then have occurred much later (Fig. 5), following regeneration of Pb by U-decay (Fig. 3c).

These data support a scenario in which an early energetic primary collision produced the light-dark textured melt breccia material, deforming, recrystallising, and damaging phosphates (Fig. 5). A late second collision then liberated the Chelyabinsk breccia as spall, low-velocity ejecta, or catastrophic fragmentation of the parent body (Fig. 5), subjecting the material to mild pressure-temperature conditions, further propagating fracture networks, and inducing Pb-loss from damaged phosphate grains. Our interpretation is consistent with evidence for enhanced Pb-loss from previously impact-metamorphosed phosphate grains[37], and from U-series disequilibria for recent impact-induced Pb mobility at mild temperatures in carbonaceous chondrites[41]. Our results support an emerging dichotomy between mechanisms of meteoritic and terrestrial apatite Pb-loss[38], with microtextures efficiently driving Pb-loss from extraterrestrial phases that largely lack common Pb[37]. Chelyabinsk phosphates record both the earliest and most energetic and most recent collision. We suggest

that the numerous intermediate ages returned by other mineral chronometers[29] may broadly represent partial resetting behaviour during the most recent collision experienced by Chelyabinsk—an effect though which phosphate U–Pb concordia ages allow us to see through clearly.

Structure of the meteoritic phosphate U–Pb record. We can further test our model for the collision history of Chelyabinsk by using it to make predictions for the wider chondritic phosphate texture-age record. We group meteorites into highly shocked (S4-6) and weakly shocked (S1-3), which corresponds to the conditions above and below the threshold for phosphate U–Pb resetting determined by Blackburn et al.[39]. If generally applicable, our model predicts that highly shocked meteorites should have fully reset upper-intercept phosphate U–Pb ages (i.e., ages younger than the parent body cooling age of circa 4500 Ma), whereas phosphates in weakly shocked meteorites will record parent body cooling (ages greater than 4500 Ma). Both highly and weakly shocked meteorites may, but do not have to, display well-defined lower intercept ages, plausibly corresponding to a recent collision experienced by an asteroid.

Compiling all published SIMS single phosphate U–Pb ages for chondritic meteorites (Fig. 6), we find support for our predictions. Our preferred upper-intercept age of 4453 ± 36 Ma lies within the 4480–4440 age peak for shocked chondrite U–Pb phosphate ages highlighted by the previous studies[9,26]. Primitive meteorites display noticeably reset upper-intercept phosphate U–Pb ages, clustering strongly at around 4480–4440 Ma (Fig. 6)[10]. The 4480–4440 Ma age cluster consists of 10 meteorites (out of 12 with published SIMS ages—Supplementary Data 2). The 4480–4440 Ma cluster is also diverse, comprising meteorites from at least 4 asteroidal parent bodies (brachinite, carbonaceous, LL, and L ordinary), ruling out simple repeat sampling of an event affecting a single parent body. Of the 6 highly shocked meteorites,
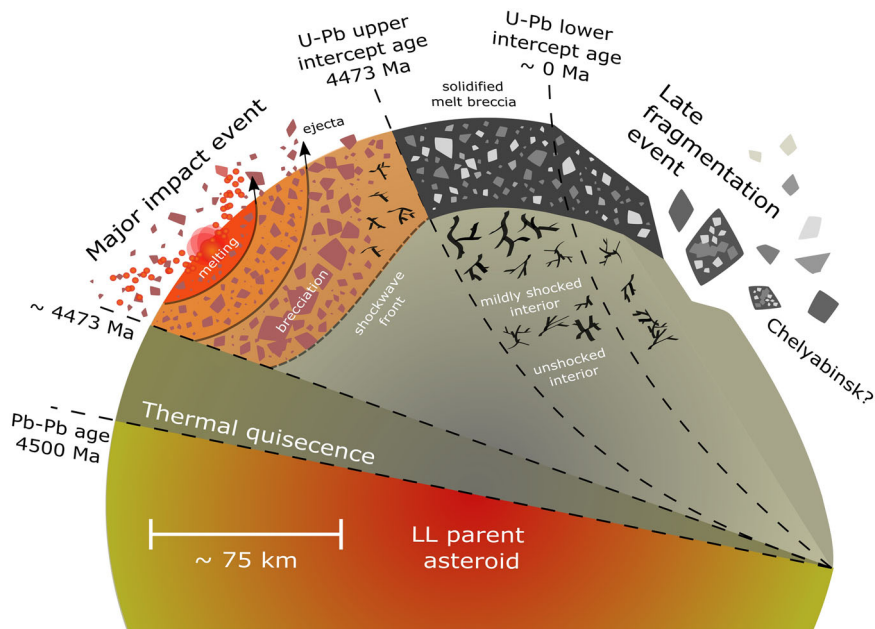
Fig. 5 Proposed formation history of the Chelyabinsk meteorite. Schematic view of collisions affecting the source material of Chelyabinsk on the LL parent body. Early radiogenic metamorphism gives way to cooling of the parent body. A primary collision locally produces shock melt at the surface of the asteroid, which cools relatively quickly (shock-induced features incompletely annealed during post-shock thermal metamorphism). A later spalling event is then needed to liberate the Chelyabinsk material from the LL parent body, and may be responsible for late Pb loss and lower intercept ages.

5 plot within the 4480–4440 Ma age cluster. This age cluster also notably contains several weakly shocked meteorites (Fig. 4b). However, several lines of evidence nonetheless link all of these ages to impact-induced metamorphism.

A plausible mechanism for producing young phosphate U–Pb upper-intercept ages in otherwise weakly shocked meteorites is being exposed to a fluid flow. Unequilibrated asteroidal material may be strongly chemically reactive during fluid flow induced by mild impact-induced heating; conditions which are suitable for phosphate nucleation and growth[42]. Thus, apparently reset phosphate U–Pb ages can be produced by new growth, requiring less extensive heating than is needed to fully diffuse Pb from a pre-existing phosphate grain. Such hydrothermal activity can occur in otherwise thermally quiescent asteroids following impact events. Looking to the specific low shock samples that plot around 4480–4440 Ma in Fig. 6b, both Dar al Gani 978, a carbonaceous chondrite, and Graves Nunataks 06128, an ungrouped achondrite of possible brachinite affinity, preserve evidence of late-stage hydrothermal activity that produced phosphates[42,43].

Conversely, especially prolonged heating may erase (anneal) textural evidence of shock in a meteorite[44]. Dishchii'bikoh, an LL7 chondrite in the 4480–4440 Ma cluster, is severely metamorphosed but displays limited shock-related features, such as thin melt veins that cross-cut primary metamorphic features[45]. However, phosphates in Dishchii'bikoh display Pb–Pb and U–Pb ages that are within error of one another (at around 4480–4440 Ma). It is therefore likely that phosphates in Dishchii'bikoh either formed or were completely stripped of Pb at 4470 Ma, corresponding to a significant thermal perturbation of the LL parent asteroid via impact at this time.

The phosphate texture-age record also contains highly shocked meteorites with older upper-intercept ages measured for host rock phosphates, compared to younger upper-intercept ages for melt-vein entrained grains, e.g., Suizhou, 4547 ± 19 for host rock phosphates versus 4481 ± 30 Ma for melt-entrained phosphates[46]. Furthermore, there are examples of weakly shocked meteorites with

upper-intercept ages consistent with radiogenic cooling, which also preserve lower intercept ages, e.g., Richardton, 4552.3 ± 3.1 Ma and 385 ± 290 Ma[47]. These pieces of evidence strongly indicate that, as in Chelyabinsk, reset upper-intercept phosphate U–Pb ages in primitive meteorites track the intense post-shock heating associated with major impacts, whereas lower intercept ages do not require such conditions to be produced[33,34,37]. Finally, we find that all reported upper and lower intercept phosphate U–Pb ages for chondritic meteorites cluster in ancient and recent Solar System history.

There are presently no examples of upper or lower intercept phosphate U–Pb ages that lie between 3 and 1 Ga reported for primitive meteorites. Given the conditions we interpret to have produced upper versus lower interpret ages, we conclude that (1) the abundance of primitive asteroidal material with fully reset phosphates, and thus the frequency of large highly energetic impact events, steeply declined after around 4440 Ma, and that (2) owing to a short residence time of material on Earth-crossing orbits, and the scarcity of fossil meteorites on Earth, there is a strong sampling bias in our collections towards more recently liberated asteroidal material, with young lower intercept ages. The L parent body disruption event is an outlier in this regard, having produced a large amount of material preserved in the fossil meteorite record[16], and which continues to fall to Earth today[9].

Implications for dating ancient and recent asteroid collisions. We have presented evidence that Chelyabinsk phosphate texture-age relationships robustly record an early energetic collision and a recent spalling event. Our interpretation of a recent spalling event involving the LL chondrite body—as revealed by Chelyabinsk phosphate U–Pb lower intercept ages and fracture-associated patchy CL textures—is also supported by evidence from Chelyabinsk Ar–Ar systematics[31] and cosmic ray exposure ages[29]. Geologically recent interaction between asteroidal parent bodies is well supported by observations of the present day asteroid belt, which suggest numerous recent (less than 50 Ma) collisions
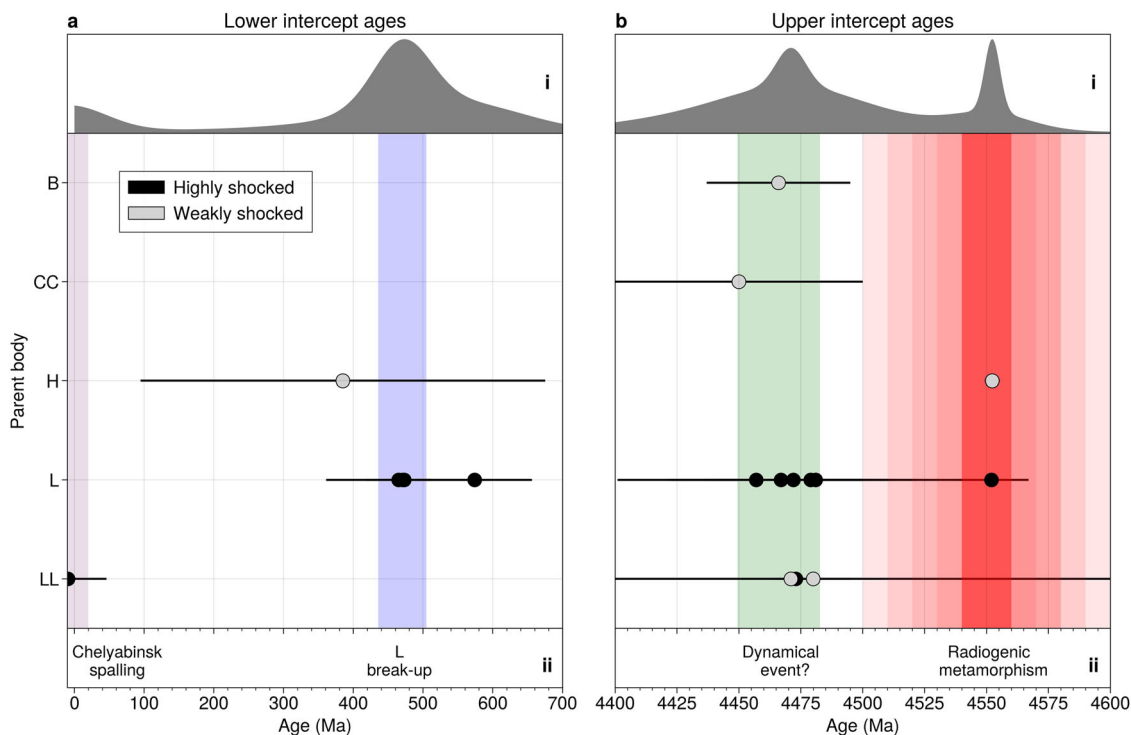
Fig. 6 Compiled shock and phosphate U–Pb age data for meteorites. In (**a**) recent Solar System history and **b** early Solar System history. **a**, **b**–**i** Stacked Gaussian probability distributions of meteorite phosphate U–Pb ages. **a**, **b**–ii Compilation of meteorites and their U–Pb phosphate ages. We divide meteorites by shock stage (see Electronic Appendix) into weakly shocked (S1-3) and highly shocked (S4-6), with the latter being sufficient for full phosphate U–Pb resetting[39]. Estimated limits for temporal range of parent body thermal metamorphism are shaded in red. Lower intercept evidence for an L-type break-up event is found at around 470 Ma, as well as a comparatively recent LL-type break-up event involving Chelyabinsk. A cluster of upper-intercept ages is clearly defined at 4480–4440 Ma, which may record a major dynamical event in the Solar System. Data from refs. [9,17,26,42,43,45,46,57–59]. Error bars are 2σ.

involving chondritic material[48–50]. Phosphate U–Pb lower intercept ages may therefore date events of some significance in recent inner Solar System collisional history.

Whilst not microtexturally constrained, the extensive dating work performed by Yin et al.[9] on the Novato L6 chondrite reveals a potentially robust lower intercept phosphate U–Pb age, defined by data lying close to the concordia, that is within error of the Ar–Ar and fossil meteorite age peak observed for meteorites from this parent body[24]. However, Ar–Ar methods both for Chelyabinsk and the wider meteorite record also return numerous ages that are not clearly evidenced in either the phosphate U–Pb system or by mineral textures (Supplementary Figs. 17, 18). It can therefore be argued that phosphate minerals offer an archive of ancient and recent thermal events that may be absent or overprinted in the Ar–Ar system. However, we cannot yet place equivalent levels of confidence in upper versus lower intercept phosphate U–Pb ages.

Our results reveal that interpreting the detailed structure of the meteoritic phosphate lower intercept U–Pb age record will require the use of microtextural constraints to sub-divide isotopic data for regression, e.g., the significantly revised lower intercept age obtained in this study in comparison to former studies of Chelyabinsk phosphates[27]. Currently published lower intercept ages that lack microtextural context must therefore be treated with some caution, especially if obtained after regressing weakly discordant data. Conversely, similar phosphate U–Pb upper-intercept ages are obtained during regression regardless of how isotopic data is sub-divided (Fig. 4). Whilst microtextural context is needed to correctly interpret the geological histories of individual meteoritic phosphates, our approach reveals that reset phosphate upper-intercept U–Pb ages are a robust archive of

ancient energetic collisions. Phosphate analyses therefore support that primitive asteroids experienced a pulse of high energy collisions between 4480–4440 Ma (Fig. 6b), which may indicate Solar System reorganisation at this time, e.g., Earth-Moon formation, or the migration of giant planets[9–11].

Overall, our results bolster the use of phosphate texture-age relationships in deciphering asteroidal collision histories, where a relative sequence of impacts can be established using mineral textures and put into chronological context using spatially resolved dating techniques. Phosphate U–Pb lower intercept ages of fracture-damaged phosphate domains emerge from our work as a valuable tool to probe recent disruption events. Here, further textural constraints on structure-chemistry relationships in damaged versus pristine phosphate grains (e.g., understanding origin of patchy CL texture around fractures) will be vital for understanding phosphate response to impact-induced metamorphism, and thus mechanisms of phosphate Pb-loss. By comparison, phosphate U–Pb upper-intercept ages in highly shocked meteorites are a remarkably robust archive of ancient and intensive collisional reheating. Determining the origin and significance of clustered upper-intercept ages will require leveraging improved phosphate U–Pb age statistics, constraints on phosphate response to shock and post-shock metamorphism, and dynamical simulations coupled to models of diffusion-driven phosphate U–Pb age resetting behaviour[7,8,39,51]. In resolving a collision history for the Chelyabinsk meteorite, we demonstrate the importance of linking textural analysis with mineral age data when tracing collisions via the meteorite record. In future, combined phosphate texture-age analysis has the potential to access and interpret detailed asteroidal chronologies of both ancient and recent Solar System evolution.

Methods

U–Pb phosphate SIMS analyses. U–Pb dating of apatite was carried out using the CAMECA IMS 1280 at the Institute of Geology and Geophysics, Chinese Academy of Sciences (IGGCAS). The O_{2-} primary ion beam was accelerated at −13.8 kV with a current of 10^{-12} nA. The Gaussian illumination mode was used in order to evenly sputter material over the analytical area. The spot diameter was 10×15 μm². Positive secondary ions were extracted with a 10 kV potential. Four magnetic field sequences were used to collect secondary ions $^{40}Ca_2^{31}P^{16}O_3^+$, $^{204}Pb^+$, $^{206}Pb^+$, $^{207}Pb^+$, $^{238}U^+$, $^{232}Th^{16}O^+$, $^{238}U^{16}O^+$ and $^{238}U^{16}O_2^+$ [52]. The $^{40}Ca_2^{31}P^{16}O_3^+$ peak was used as a reference peak for centreing the secondary ion beam as well as for making energy and mass adjustments. NW-1 apatite standard (1160 ± 5 Ma) was used for U–Pb fractionation calibration[52] and ages were calculated using IsoplotR[52,53]. Further details can be found in[54]. We identified fracture-damaged versus pristine phosphate domains using SEM BSE + CL images (see Supplementary Information Figs. 1–9).

Compilation of meteorite shock age/stage data. Textural evidence of shock is often classified using the shock stage scheme[55,56], and provides some context for age data obtained using a given sample. We performed a comprehensive survey of meteorite shock ages and shock stages. We report age uncertainties to 2 σ. Where shock stages were not directly reported in the meteorite, or where conflicting shock stages were assigned, we applied a simple set of classification rules: (1) petrologic type 7 and impact-melt samples are assigned shock stage 6 (highest possible), (2) more recent classifications take precedence, (3) samples with some noted presence of shock darkening and melt veins are cautiously assigned shock stage 3 (moderate shock), (4) samples with extensive but not complete development of shock melt (i.e., S4-6 samples, such as Chelyabinsk) are given a single shock stage classification of 5. We then group meteorites into highly shocked (S4-6) and weakly shocked (S1-3), which corresponds to the conditions above and below the threshold for phosphate U–Pb resetting determined by Blackburn et al.[39]. This approach simplifies visual presentation of the shocked meteorite record. We note that the formal guidance for assignment and interpretation of meteorite shock stages has varied over time[19,55]. However, our compilation broadly includes recently studied meteorites, for which shock stages assignment may differ only subtly in the literature (e.g., reference to Chelyabinsk as an S4–6, or S5, meteorite). Thus, the essential features of the record are robust in the face of minor disagreements on meteorite shock stage assignments in the literature.

Data availability

All data published in this manuscript are available as a part of the supplementary information files, and in Supplementary Data files 1 and 2. These data have been deposited in the National Geoscience Data Centre (NGDC), accessible with the search terms Chelyabinsk and NE/L002507/1.

References

1. Kobayashi, H., Tanaka, H. & Okuzumi, S. From planetesimals to planets in turbulent protoplanetary disks. I. Onset of runaway growth. *Astrophys. J.* **817**, 105 (2016).
2. Genda, H. & Abe, Y. Enhanced atmospheric loss on protoplanets at the giant impact phase in the presence of oceans. *Nature* **433**, 842 (2005).
3. Schulte, P. et al. The Chicxulub asteroid impact and mass extinction at the Cretaceous-Paleogene boundary. *Science* **327**, 1214–1218 (2010).
4. Cattermole, P. Melosh, H. J. 1996. Impact cratering. a geologic process. Oxford Monographs on Geology and Geophysics no. 11. First paperback edition; first published 1989. 254pp. New York, Oxford: Oxford University Press. Price £27.95 (paperback). *Geol. Mag.* **134**, 269–281 (1997).
5. Moser, D. E. et al. Decline of giant impacts on Mars by 4.48 billion years ago and an early opportunity for habitability. *Nat. Geosci.* **12**, 522–527 (2019).
6. Boehnke, P. & Harrison, T. M. Illusory late heavy bombardments. *Proc. Natl Acad. Sci.* **113**, 10802–10806 (2016).
7. Bottke, W. F. et al. Dating the Moon-forming impact event with asteroidal meteorites. *Science* **348**, 321–323 (2015).
8. Edwards, G. H. & Blackburn, T. Accretion of a large LL parent planetesimal from a recently formed chondrule population. *Sci. Adv.* **6**, eaay8641 (2020).
9. Yin, Q. et al. Records of the Moon-forming impact and the 470 Ma disruption of the L chondrite parent body in the asteroid belt from U-Pb apatite ages of Novato (L6). *Meteoritics. Planet. Sci.* **49**, 1426–1439 (2014).
10. Mojzsis, S. J., Brasser, R., Kelly, N. M., Abramov, O. & Werner, S. C. Onset of giant planet migration before 4480 million years ago. *Astrophys. J.* **881**, 44 (2019).
11. Marchi, S. et al. High-velocity collisions from the lunar cataclysm recorded in asteroidal meteorites. *Nat. Geosci.* **6**, 303 (2013).
12. Marchi, S. et al. Widespread mixing and burial of Earth's Hadean crust by asteroid impacts. *Nature* **511**, 578 (2014).
13. Mazrouei, S., Ghent, R. R., Bottke, W. F., Parker, A. H. & Gernon, T. M. Earth and Moon impact flux increased at the end of the Paleozoic. *Science* **363**, 253–257 (2019).
14. Alexeev, V. A. Parent bodies of L and H chondrites: times of catastrophic events. *Meteoritics Planet. Sci.* **33**, 145–152 (1998).
15. Heck, P. R. et al. Rare meteorites common in the Ordovician period. *Nat. Astron.* **1**, 0035 (2017).
16. Schmitz, B. et al. An extraterrestrial trigger for the mid-Ordovician ice age: dust from the breakup of the L-chondrite parent body. *Sci. Adv.* **5**, eaax4184 (2019).
17. Li, Y. & Hsu, W. Multiple impact events on the L-chondritic parent body: Insights from SIMS U-Pb dating of Ca-phosphates in the NWA 7251 L-melt breccia. *Meteoritics. Planet. Sci.* **53**, 1081–1095 (2018).
18. Morlok, A., Bischoff, A., Patzek, M., Sohn, M. & Hiesinger, H. Chelyabinsk—a rock with many different (stony) faces: an infrared study. *Icarus* **284**, 431–442 (2017).
19. Stöffler, D., Hamann, C. & Metzler, K. Shock metamorphism of planetary silicate rocks and sediments: Proposal for an updated classification system. *Meteoritics & Planetary Science* **53**, 5–49 (2018).
20. Bischoff, A., Scott, E. R. D., Metzler, K. & Goodrich, C. A. In *Meteorites and the Early Solar System II* (eds. Lauretta, D. S. & McSween, H.Y. Jr.) 79–712 (Univ. of Arizona Press, 2006).
21. Walton, C. R. et al. Microtextures in the Chelyabinsk impact breccia reveal the history of Phosphorus-Olivine-Assemblages in chondrites. *Meteorit. Planet. Sci.* **56**, 742–766 (2021).
22. Moreau, J.-G., Kohout, T. & Wünnemann, K. Melting efficiency of troilite-iron assemblages in shock-darkening: insight from numerical modeling. *Phys. Earth. Planet. Interiors* **282**, 25–38 (2018).
23. Moreau, J.-G. & Schwinger, S. Heat diffusion in numerically shocked ordinary chondrites and its contribution to shock melting. *Phys. Earth. Planet. Interiors* **310**, 106630 (2021).
24. Korochantseva, E. V. et al. Ar–Ar dating L chondrites. *Meteorit. Planet. Sci.* **42**, 113–130 (2007).
25. Kenny, G. G. et al. Recrystallization and chemical changes in apatite in response to hypervelocity impact. *Geology* **48**, 19–23 (2019).
26. Lapen, T. J. et al. Uranium-lead isotope evidence in the chelyabinsk ll5 chondrite meteorite for ancient and recent thermal events. In: *45th Lunar and Planetary Science Conference* (2014).
27. Popova, O. P. et al. Chelyabinsk airburst, damage assessment, meteorite recovery, and characterization. *Science* **342**, 1069–1073 (2013).
28. Bogomolov, E. S. et al. Sm-Nd age and isotope geochemistry of minerals of the Chelyabinsk meteorite. *Dokl. Earth Sci.* **452**, 1034–1038 (2013).
29. Righter, K. et al. Mineralogy, petrology, chronology, and exposure history of the Chelyabinsk meteorite and parent body. *Meteorit. Planet. Sci.* **50**, 1790–1819 (2015).
30. Lindsay, F. N. et al. Chelyabinsk Ar ages—a young heterogeneous LL5 chondrite. In: *46th Lunar and Planetary Science Conference* Abstract #2226 (2015).
31. Beard, S. P., Kring, D. A., Isachsen, C. E. & Lapen, T. J. Ar–Ar analysis of chelyabinsk: evidence for a recent impact. In: *45th Lunar and Planetary Science Conference* (2014).
32. Mezger, K. & Krogstad, E. J. Interpretation of discordant U-Pb zircon ages: an evaluation. *J. Metamorphic Geol.* **15**, 127–140 (1997).
33. McGregor, M., McFarlane, C. R. & Spray, J. G. In situ LA-ICP-MS apatite and zircon U-Pb geochronology of the Nicholson Lake impact structure, Canada: shock and related thermal effects. *Earth Planet. Sci. Lett.* **504**, 185–197 (2018).
34. McGregor, M., McFarlane, C. R. M. & Spray, J. G. In situ multiphase U-Pb geochronology and shock analysis of apatite, titanite and zircon from the Lac La Moinerie impact structure, Canada. *Contrib. Mineral. Petrol.* **174**, 62 (2019).
35. Cox, M. A. et al. High-resolution microstructural and compositional analyses of shock deformed apatite from the peak ring of the Chicxulub Impact Crater. *Meteorit. Planet. Sci.* https://doi.org/10.1111/maps.13541 (2020).
36. White, L. F., Darling, J., Dunlop, J., Anand, M. & Cernok, A. Shock-induced microtextures in lunar apatite and merrillite. *Meteorit. Planet. Sci.* **54**, 1262–1282 (2019).
37. Černok, A. et al. Lunar samples record an impact 4.2 billion years ago that may have formed the Serenitatis Basin. *Commun. Earth Environ.* **2**, 120 (2021).
38. McGregor, M., Erickson, T. M., Spray, J. G. & Whitehouse, M. J. High-resolution EBSD and SIMS U-Pb geochronology of zircon, titanite, and apatite: insights from the Lac La Moinerie impact structure, Canada. *Contrib. Mineral. Petrol.* **176**, 76 (2021).

39. Blackburn, T., Alexander, C. M., Carlson, R. & Elkins-Tanton, L. T. The accretion and impact history of the ordinary chondrite parent bodies. *Geochim. Cosmochim. Acta* **200**, 201–217 (2017).

40. Herrmann, M. et al. The effect of low-temperature annealing on discordance of U-Pb zircon ages. *Sci. Rep.* **11**, 7079 (2021).

41. Turner, S., McGee, L., Humayun, M., Creech, J. & Zanda, B. Carbonaceous chondrite meteorites experienced fluid flow within the past million years. *Science* **371**, 164–167 (2021).

42. Zhang, A.-C. et al. Young asteroidal fluid activity revealed by absolute age from apatite in carbonaceous chondrite. *Nat. Commun.* **7**, 12844 (2016).

43. Zhou, Q. et al. U-Pb and Pb-Pb apatite ages for Antarctic achondrite Graves Nunataks 06129. *Meteorit. Planet. Sci.* **53**, 448–466 (2018).

44. Rubin, A. E. Postshock annealing and postannealing shock in equilibrated ordinary chondrites: Implications for the thermal and shock histories of chondritic asteroids. *Geochim. Cosmochim. Acta* **68**, 673–689 (2004).

45. Jenniskens, P. et al. Orbit and origin of the LL7 chondrite Dishchii'bikoh (Arizona). *Meteorit. Planet. Sci.* **55**, 535–557 (2020).

46. Li, S. & Hsu, W. Dating phosphates of the strongly shocked Suizhou chondrite. *Am. Mineralogist* **103**, 1789–1799 (2018).

47. Amelin, Y., Ghosh, A. & Rotenberg, E. Unraveling the evolution of chondrite parent asteroids by precise U-Pb dating and thermal modeling. *Geochim. Cosmochim. Acta* **69**, 505–518 (2005).

48. Farley, K. A., Vokrouhlický, D., Bottke, W. F. & Nesvorný, D. A late Miocene dust shower from the break-up of an asteroid in the main belt. *Nature* **439**, 295–297 (2006).

49. Greenwood, R. C., Burbine, T. H. & Franchi, I. A. Linking asteroids and meteorites to the primordial planetesimal population. *Geochim. Cosmochim. Acta* **277**, 377–406 (2020).

50. Nesvorný, D., W. F., B. Jr, Dones, L. & Levison, H. F. The recent breakup of an asteroid in the main-belt region. *Nature* **417**, 720–721 (2002).

51. Davison, T. M., O'Brien, D. P., Ciesla, F. J. & Collins, G. S. The early impact histories of meteorite parent bodies. *Meteorit. Planet. Sci.* **48**, 1894–1918 (2013).

52. Li, Q.-L. et al. In-situ SIMS U-Pb dating of phanerozoic apatite with low U and high common Pb. *Gondwana Res.* **21**, 745–756 (2012).

53. Vermeesch, P. IsoplotR: a free and open toolbox for geochronology. *Geosci. Frontiers* **9**, 1479–1493 (2018).

54. Zhou, Q. et al. Geochronology of the Martian meteorite Zagami revealed by U-Pb ion probe dating of accessory minerals. *Earth Planet. Sci. Lett.* **374**, 156–163 (2013).

55. Stöffler, D., Keil, K. & R.D, S. E. Shock metamorphism of ordinary chondrites. *Geochim. Cosmochim. Acta* **55**, 3845–3867 (1991).

56. Fritz, J., Greshake, A. & Fernandes, V. A. Revising the shock classification of meteorites. *Meteorit. Planet. Sci.* **52**, 1216–1232 (2017).

57. Wu, Y. & Hsu, W. Petrogenesis and in situ U-Pb geochronology of a strongly shocked L-melt rock Northwest Africa 11042. *J. Geophys. Res.: Planets* **124**, 893–909 (2018).

58. Ozawa, S. et al. Shock metamorphism of L6 chondrites Sahara 98222 and Yamato 74445: the PT conditions and the shock age. *AGU Fall Meeting Abstr.* MR43B–1234 (2007).

59. Terada, K. & Bischoff, A. Asteroidal granite-like magmatism 4.53 Gyr ago. *Astrophys. J.* **699**, L68–L71 (2009).

Author contributions
C.R.W. conceived of the project, performed electron microscopy, analysed U–Pb data, and wrote the manuscript. S.H. and J.J. performed U–Pb SIMS analyses. A.C gathered and processed EBSD data. O.S., A.S.P.R., H.W., G.T., Q.L., Y.L. and M.A. contributed to the editing of the manuscript and advisory aspects of the project.

Competing interests
The authors declare no competing interests.

Additional information
Supplementary information The online version contains supplementary material available at https://doi.org/10.1038/s43247-022-00373-1.

Correspondence and requests for materials should be addressed to Craig R. Walton.

Peer review information *Communications Earth & Environment* thanks the anonymous reviewers for their contribution to the peer review of this work. Primary Handling Editor: Joe Aslin. Peer reviewer reports are available.

Reprints and permission information is available at http://www.nature.com/reprints

Publisher's note Springer Nature remains neutral with regard to jurisdictional claims in published maps and institutional affiliations.